We are IntechOpen,
the world's leading publisher of
Open Access books
Built by scientists, for scientists

6,900
Open access books available

185,000
International authors and editors

200M
Downloads

154
Countries delivered to

Our authors are among the

TOP 1%
most cited scientists

12.2%
Contributors from top 500 universities

BOOK
CITATION
INDEX
CLARIVATE ANALYTICS
INDEXED

WEB OF SCIENCE™

Selection of our books indexed in the Book Citation Index
in Web of Science™ Core Collection (BKCI)

Interested in publishing with us?
Contact book.department@intechopen.com

Hexagonal vs Circular Cell Shape: A Comparative Analysis and Evaluation of the Two Popular Modeling Approximations

Konstantinos B. Baltzis
Aristotle University of Thessaloniki
Greece

1. Introduction

Recent years have witnessed an explosion in wireless communications. In the last decades, the development of wireless communication systems and networks is taking us from a world where communications were mostly carried over PSTN, packet-switched and high speed LAN networks to one where the wireless transmission dominates. Nowadays, high data rates carry multimedia communications, real-time services for delay-sensitive applications are added and networks are asked to deal with a traffic mix of voice, data and video. Next generation mobile systems will further include a variety of heterogeneous access technologies, support multimedia applications and provide end-to-end IP connectivity (Bolton et al., 2007; Xylomenos et al., 2008; Demestichas et al., 2010). Undoubtedly, new possibilities are created for both telcos and users and important design and traffic issues emerge. This revolution has spurred scientists toward the development of reliable and computationally efficient models for evaluating the performance of wireless networks.

A crucial parameter in the modeling of a cellular communication system is the shape of the cells. In real life, cells are irregular and complex shapes influenced by terrain features and artificial structures. However, for the sake of conceptual and computational simplicity, we often adopt approximate approaches for their design and modeling. In the published literature, cells are usually assumed hexagons or circles. The hexagonal approximation is frequently employed in planning and analysis of wireless networks due to its flexibility and convenience (Jan et al., 2004; Goldsmith, 2005; Pirinen, 2006; Chan & Liew, 2007; Hoymann et al., 2007; Baltzis, 2008, 2010a; Choi & You, 2008; Dou et al., 2008; Xiao et al., 2008; Baltzis & Sahalos, 2010). However, since this geometry is only an idealization of the irregular cell shape, simpler models are often used. In particular, the circular–cell approximation is very popular due to its low computational complexity (Petrus et al., 1998; Baltzis & Sahalos, 2005, 2009b; Goldsmith, 2005; Pirinen, 2006; Bharucha & Haas, 2008; Xiao et al., 2008; Baltzis, 2010b).

Among various performance degradation factors, co-channel interference (CCI) is quite significant since the cells in cellular networks tend to become denser in order to increase system capacity (Stavroulakis, 2003). The development of models that describe CCI generates great interest at the moment. Several reliable models can be found in the

published literature (Butterworth et al., 2000; Cho et al., 2000; Cardieri & Rappaport, 2001; Zhou et al., 2003; Grant and Cavers, 2004; Masmoudi and Tabbane, 2006). However, their practical application is restricted by their algorithmic complexity and computational cost, which results in the development of simpler models. A simplified approach is the geometrical-based modeling that allows an approximate but adequate evaluation of system performance (Petrus et al., 1998; Au et al. 2001; Zhang et al., 2004, 2006; Baltzis & Sahalos, 2005, 2009b, 2010; Panagopoulos et al., 2007; Baltzis, 2008).

Another important issue in the study of a wireless system is the prediction of signal attenuation (Parsons, 2000; Fryziel et al. 2002; Baltzis, 2009). In general, path loss models approximate signal attenuation as a function of the distance between communicating nodes. The majority of the developed models are based on empirical measurements over a given distance in a specific frequency range and a particular environment (Ghassemzadeh, 2004; Moraitis and Constantinou, 2004; Holis and Pechac, 2008). However, the application of these models is not recommended in general environments because they are closely related to network and environmental parameters. Therefore, several other methods have been further developed for the description of path loss. For example, Haenggi introduced a unified framework that allowed the geometric characterization of fading (Haenggi, 2008). Proposals based on neural network techniques are also of great interest (Cerri et al. 2004, Popescu et al., 2006; Östlin et al., 2010). Approximate analytical methods that reduce significantly the computational requirements and the cost of the simulations can also be found in the published literature (Bharucha & Haas, 2008; Baltzis, 2010a,b).

In this chapter, we discuss and evaluate the hexagonal and the circular cell shape modeling approximations in a cellular network. The analysis focuses on the impact of the shape of the cells on co-channel interference and path loss attenuation. First, we present three two-dimensional geometrical-based models for the Angle-of-Arrival (AoA) of the uplink interfering signals in a cellular system and their application in the study of co-channel interference. Next, we present analytical and approximate closed-form expressions for the path loss statistics in cellular networks with hexagonal and circular cells; the role of cell shape in signal level is explored by representative examples.

The chapter proceeds as follows: Section 2 highlights some theoretical background on the hexagonal and the circular cell shape approximations. Then we study the impact of cell shape on performance degradation due to co-channel interference and on RF signal attenuation. In particular, Section 3 provides and evaluates some geometrical-based models for the description of co-channel interference in cellular networks with circular or hexagonal cells and Section 4 discusses the statistics of path loss in these systems. Finally, some research ideas are conclusions are pointed out.

2. The approximations of the hexagonal and the circular cell

Cellular networks are infrastructure-based networks deployed throughout a given area. One of their features is the efficient utilization of spectrum resources due to frequency reuse. In practice, frequency reuse is a defining characteristic of cellular systems. It exploits the fact that signal power falls of with distance to reuse the same frequency spectrum at spatially separated locations (cells).

In a cellular communication system, cell shape varies depending on geographic, environmental and network parameters such as terrain and artificial structures properties, base station location and transmission power, accessing techniques, etc. Nevertheless, for

representation and analytical simplicity, cells are usually approximated as regular shapes such as hexagons and circles. In the following paragraphs, we will discuss the main features of the two approximations. The interested reader can consult the published literature for further information (MacDonald, 1979; Kim, 1993; Lee and Miller, 1998).

A hexagon is a tessellating cell shape in that cells can be laid next to each other with no overlap; therefore, they can cover the entire geographical region without any gaps. This approximation is frequently employed in planning and analysis of cellular networks. In practice, hexagons are commonly used to approximate cell shapes in macrocellular systems with base stations placed at the top of buildings (Goldsmith, 2005). Figure 1 shows a typical hexagonal cell layout with frequency reuse factor seven. Cells are numbered according to the frequency band they use. In this figure, we further depict the desired cell (red-colored), the six equidistant nearest interfering cells, i.e. the first ring of cells that use the same spectrum resources (grey-colored), and the second tier of interferers (black-colored).
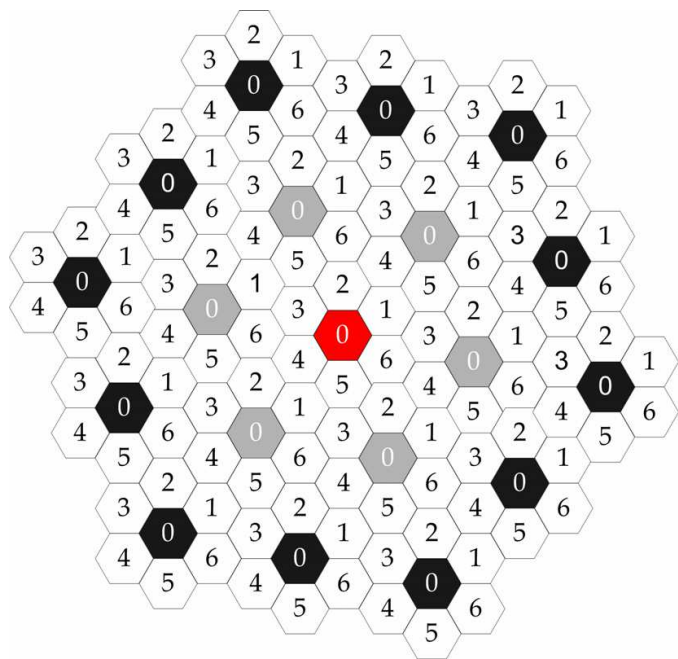

Fig. 1. Hexagonal cell layout.

A simpler assumption, the circular-shaped cell, is also common in the literature. A reasonable approximation of this assumption is provided when signal propagation follows path loss models that consider constant signal power level along a circle around the base station (Goldsmith, 2005). In fact, an omni-directional base station antenna may cover a circular area that is defined as the area for which the propagating downlink signal exceeds a certain threshold; however, even in this case, this is only an approximation due to the impact of the environment. The major drawback of the circular approximation is that circular cells must partially overlap in order to avoid gaps. Examples of simple layouts are depicted in Fig. 2. Figure 2a illustrates the hexagonal cell layout. The inradius and the circumradius of the hexagonal cell are r and a, respectively. In Fig. 2b, the radius of the circular cell R equals to r; as a result, the cells do not cover the whole network coverage area. In Fig. 2c, cells are partially overlapped because R equals to the hexagon's circumradius. In this case, the model considers nodes not belonging to the cell of interest. In the next sections, the impact of cell shape on the estimation of specific performance metrics is discussed.
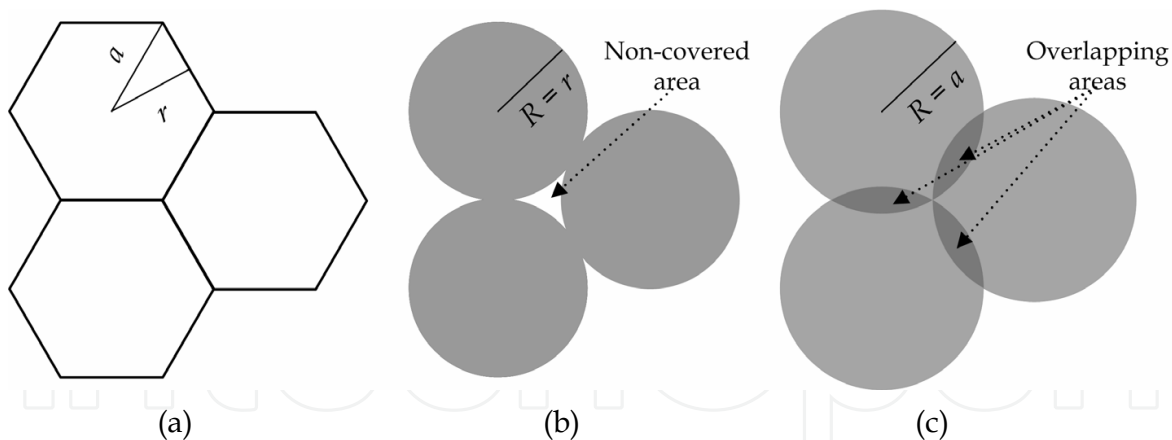
Fig. 2. Hexagonal cell layout (a) and idealized circular coverage areas (b), (c).

3. The impact of the shape of the cells on co-channel interference analysis

In this section, we explore the relation between co-channel interference and cell shape. A common measure of performance degradation due to CCI is the probability an interferer from another cell is causing interference to the cell of interest. We present three 2-D geometrical-based models for the description of the probability of uplink interference that assume circular and hexagonal cells. At this point, we have to notice that two-dimensional modeling is adequate for the description of the azimuth angular spreading of the propagating signals but fails to describe any signal variations in the elevation plane (Fuhl et al., 1997; Kuchar et al., 2000; Baltzis & Sahalos, 2009a, b; Nawaz et al., 2010).

In the development of the models, certain assumptions have been made. The base stations (BSs) are located at the centers of the cells and the mobile users (MUs) are uniformly distributed within each cell. The models assume a single line–of–sight signal path between the interferers and the BS and they consider only the first ring of co–channel interferers. They also assume that the interference power is much larger than the thermal noise power (interference-limited environment), the BS main beam points to the direction of the desired user and the transmitted BS power is maximized according to the desired user with no concern of the others.

In the circular-cell approach (Petrus et al., 1998), see Fig. 3, the cells are circles with radius R. BS_0 and BS_i are the base stations at the desired and an interfering cell, respectively. MUs are uniformly distributed within the cell; therefore, the area within the shaded region is proportional to the probability of the AoA of the uplink interfering signals.
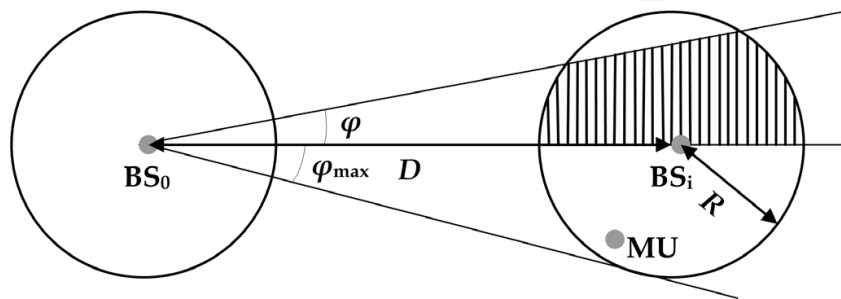

Fig. 3. The circular model.

In this case, the cdf of the AoA of the uplink interfering signals equals to the area of the shaded region multiplied by the user density. Its differentiation with respect to φ gives the corresponding pdf

$$f(\phi) = \frac{2D\cos\phi}{\pi R^2} \sqrt{R^2 - D^2 \sin^2 \phi} \, \mathrm{U}\left(\sin^{-1}\left(\frac{R}{D}\right) - |\phi| \right) \tag{1}$$

where $\mathrm{U}(\cdot)$ is the unit step function.

A method for hexagonal–shaped cells was provided by Baltzis (Baltzis, 2008). In that proposal, the probability of the AoA of the uplink interfering signals was proportional to the area of the polygon defined from the line that connected the BSs of the cell of interest and the interfering cell, the line segment determined from the angle ϕ, and the boundaries of the interfering cell, see Fig. 4.
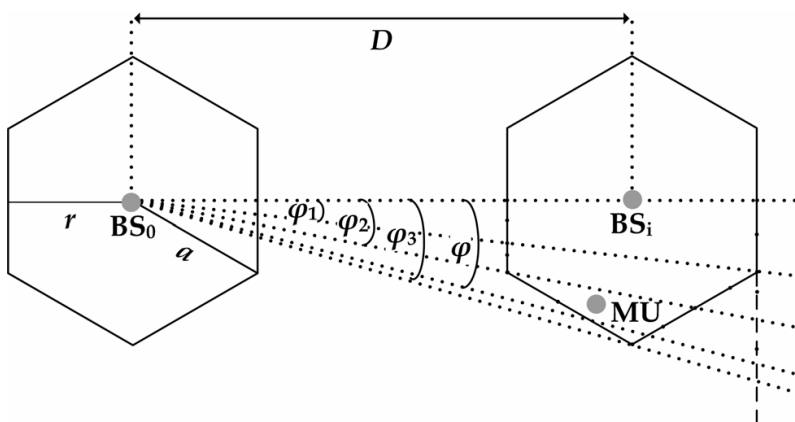

Fig. 4. The single cluster hexagonal model.

The pdf of the AoA of the uplink interfering signals is given by the expression

$$f(\phi) = \begin{cases} \dfrac{D}{\sqrt{3}r\cos^2\phi} & |\phi| \le \phi_1 \\[3ex] \dfrac{1}{\cos^2\phi}\left(\dfrac{D}{\sqrt{3}r} - \dfrac{\left(\tan|\phi| - \tan\phi_1\right)(D+r)^2\left[2 + \sqrt{3}\left(\tan|\phi| + \tan\phi_1\right)\right]}{4r^2\left(1 + \sqrt{3}\tan|\phi|\right)^2} \right), & \phi_1 \le |\phi| \le \phi_2 \\[3ex] \dfrac{\left[r + \sqrt{3}(D+r)\tan\phi_1 - \sqrt{3}D\tan|\phi|\right]\left\{D - \sqrt{3}\left[r + \sqrt{3}(D+r)\tan\phi_1\right]\tan|\phi|\right\}}{\sqrt{3}r^2\left(1 - 3\tan^2\phi\right)^2\cos^2\phi}, & \phi_2 \le |\phi| \le \phi_3 \\[3ex] 0, & |\phi| > \phi_3 \end{cases} \tag{2}$$

where

$$\phi_i = \cot^{-1}\left(\frac{\sqrt{3}D}{\mu_i r} + v_i \right), \quad i = 1,2,3 \tag{3}$$

with $\mu_{1..3} = \{1,1,2\}$ and $v_{1..3} = \{\sqrt{3}, -\sqrt{3}, 0\}$.

The model is valid for single cluster networks or topologies in which the closest edges of the two cells are properly aligned, e.g. CDMA and WCDMA networks, OFDMA systems or

special cases of ad hoc networks (Almers et al., 2007; Andrews et al., 2007; Webb, 2007; Lu et al., 2008).

Recently (Baltzis and Sahalos, 2010), the previous model was extended and included networks with hexagonal cells of arbitrary cluster size and orientation. In that proposal, the boundaries of the hexagonal cell were expressed in polar coordinates with origin the position of the desired BS, see Fig. 5, (with no loss of generality, the circumradius of the hexagon was normalized to unity) as

$$
\begin{aligned}
\rho_{\substack{(1)\\(4)}}(\phi) &= \frac{D\cos\phi_0 - \sqrt{3}\left(D\sin\phi_0 \mp 1\right)}{\cos\phi - \sqrt{3}\sin\phi} \\[2mm]
\rho_{\substack{(2)\\(5)}}(\phi) &= \frac{D\cos\phi_0 \pm \sqrt{3}/2}{\cos\phi} \\[2mm]
\rho_{\substack{(3)\\(6)}}(\phi) &= \frac{D\cos\phi_0 + \sqrt{3}\left(D\sin\phi_0 \pm 1\right)}{\cos\phi + \sqrt{3}\sin\phi}
\end{aligned}
\tag{4}
$$

under the constraint

$$
\left|\rho_{(i)}(\phi) - D\cos(\phi - \phi_0)\right| \leq \sqrt{1 - D^2 \sin^2(\phi - \phi_0)}, \quad i = 1..6
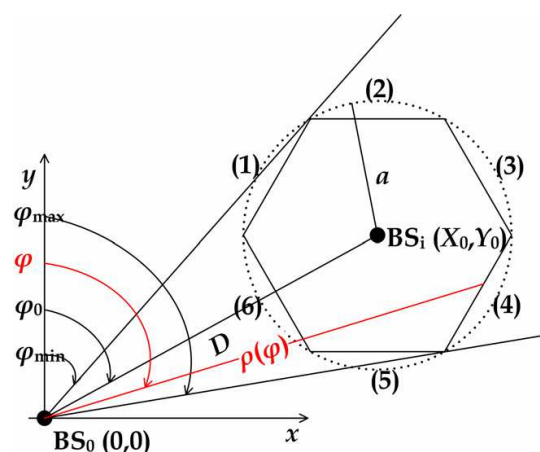\tag{5}
$$

Fig. 5. Geometry of the generalized hexagonal model.

The pdf of the AoA of the uplink interfering signals is

$$
f(\phi) = \frac{\rho_2^2(\phi) - \rho_1^2(\phi)}{3\sqrt{3}} U\left(\phi + |\phi_{\min}|\right) U\left(\phi_{\max} - \phi\right)
\tag{6}
$$

where the angles $\phi_{\min}$ and $\phi_{\max}$ depend on system geometry and

$$
\rho_1(\phi) = \max_{i=5,6}\left\{\rho_{(i)}(\phi)\right\}
\tag{7}
$$

$$
\rho_2(\phi) = \min_{i=1..4}\left\{\rho_{(i)}(\phi)\right\}
\tag{8}
$$

Next, we provide representative examples to demonstrate the efficacy of the aforementioned models. Our discussion is mainly focused on the analysis of the impact of cell shape on

system performance. Figures 6 and 7 illustrate the pdfs and cdfs of the AoA of the uplink interfering signals for cellular systems with frequency reuse factor, *K*, one, three and seven.
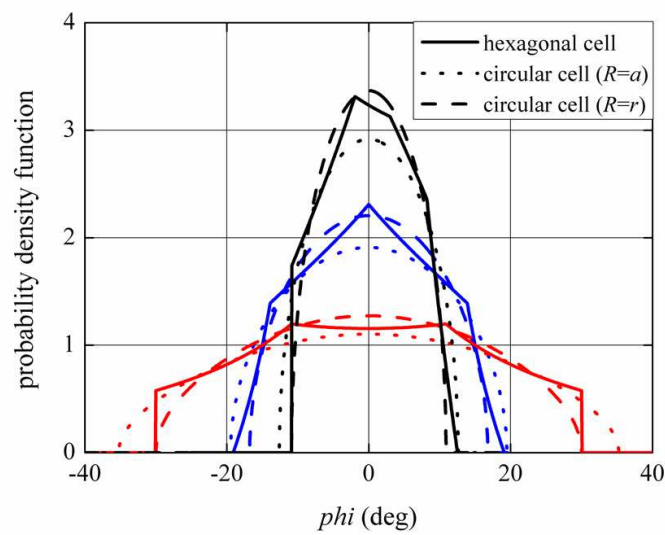

Fig. 6. Pdf of the AoA of the uplink interfering signals; the frequency reuse factor is seven (black curves), three (blue curves) and one (red curves).
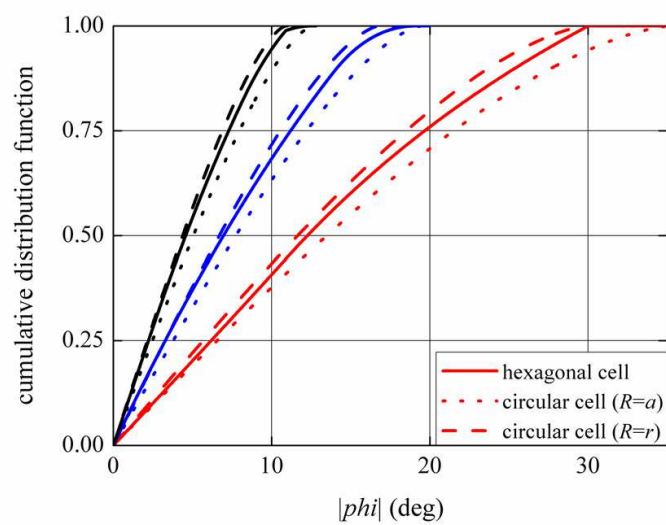

Fig. 7. Cdf of the AoA of the uplink interfering signals; the frequency reuse factor is seven (black curves), three (blue curves) and one (red curves).

Figure 6 shows that the circular and the hexagonal cell pdfs differ for small values of ϕ. In the first case, the pdfs are even functions maximized at $\phi = 0$. On the other hand, the hexagonal model for frequency reuse factor one or seven estimates the maxima of the pdfs at $\phi \neq 0$; moreover, when *K* = 7 the pdf curve is no longer symmetric with respect to $\phi = 0$. Differences are also observed at large values of ϕ. These differences are related to the different size of the cells (obviously, a circular cell with radius equal to the hexagon's inradius (circumradius) has a smaller (greater) coverage area compared to the hexagonal

cell) and their relative positions in the cluster. Noticeable differences are also observed between the cdf curves, see Fig. 7. In comparison with the hexagonal approach, the inradius (circumradius) approximation overestimates (underestimates) the amount of interference at small angles. In general, the inradius approximation gives results closer to the hexagonal solution compared with the circumradius one.

For a given azimuth angle, the probability that the users of another cell interfere with the desired uplink signal is given by the convolution of the desired BS antenna radiation pattern with the pdf of the AoA of the incoming interfering signals. The summation of all the possible products of the probability that n cells are interfering by the probability that the remaining $N - n$ do not gives the probability that n out of the possible N interfering cells are causing interference over ϕ (Petrus et al., 1998; Baltzis & Sahalos, 2005, 2009b).

Let us assume a single cluster WCDMA network with a narrow beam BS antenna radiation pattern and a three– and six–sectored configuration. The BS antenna radiation patterns are cosine–like with side lobe level –15 dB and half–power beamwidth 10, 65, and 120 degrees, respectively (Czylwik & Dekorsy, 2004; Niemelä et al., 2005). Figure 8 depicts the probability that an interfering cell causes interference over $|\phi|$ in the network (in a single cluster system, this probability is even function). We observe differences between the hexagonal and the circular approaches for small angles and angles that point at the boundaries of the interfering cell. Increase in half-power beamwidth reduces the difference between the models but increases significantly the probability of interference.
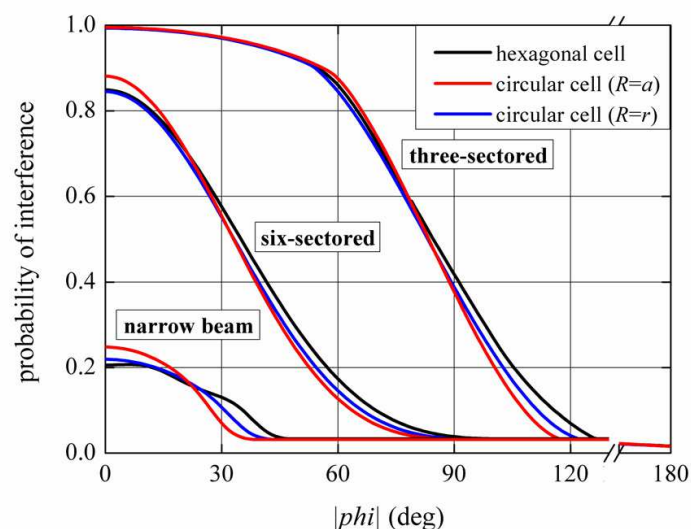

Fig. 8. Probability that an interfering cell is causing interference over $|\phi|$.

The validation of the previous models using simulation follows. The pdfs in (1) and (6) are calculated for a single cluster size WCDMA network. The users are uniformly distributed within the hexagonal cells; therefore, user density is (Jordan et al., 2007)

$$p(x,y) = \frac{1}{3ar} U(a - |x|) U(r - |y|) U(2r - |\sqrt{3}x + y|) \tag{9}$$

considering that the center of the cell is at (0,0). System parameters are as in Aldmour et al. (Aldmour et al., 2007). In order to generate the random samples, we employ the DX-120-4

pseudorandom number generator (Deng & Xu, 2003) and apply the rejection sampling method (Raeside, 1976). The simulation results are calculated by carrying out 1000 Monte Carlo trials. Table I presents the mean absolute, e_p, and mean relative, ε_p, difference between the theoretical pdf values and the simulation results (estimation errors). The simulation results closely match the theoretical pdf of (6); however, they differ significantly from the circular-cell densities. A comparison between the inradius and the circumradius approximations shows the improved accuracy of the first.

Hexagonal model		Circular model			
		$R = r$		$R = a$	
e_p	ε_p	e_p	ε_p	e_p	ε_p
1.48%	1.87%	8.17%	10.40%	9.76%	20.36%

Table 1. Probability density function: Estimation errors.

Among the measures of performance degradation due to CCI, a common one is the probability an interferer is causing interference at the desired cell. Table 2 lists the mean absolute, e_P, and mean relative, ε_P, difference between theoretical values and simulations results, i.e. the estimation error, of this probability. We consider a six–sectored and a narrow–beam system architecture. The rest of the system parameters are set as before. In the six–sectored system, we observe a good agreement between the theoretical values and the simulation results for all models. However, in the narrow–beam case, noticeable differences are observed. Again, the circumradius approximation gives the worst results.

System architecture	Hexagonal model		Circular model			
			$R = r$		$R = a$	
	e_P	ε_P	e_P	ε_P	e_P	ε_P
six–sectored system	0.59%	1.18%	1.34%	2.03%	1.86%	2.54%
narrow–beam system	0.47%	2.51%	1.19%	5.77%	3.99%	19.35%

Table 2. Probability of interference: Estimation errors.

Use of the previous models allows the approximate calculation of the co-channel interference in a cellular network. By setting CIR the Carrier–to–Interference Ratio, Q the Protection ratio, Z_d the Carrier–to–Interference plus Protection Ratio ($CIRP$), $P(n)$ the average probability that n out of the possible N interfering cells are causing interference over ϕ and $P(Z_d < 0 | n)$ the conditional probability of outage given n interferers, this term depends on fading conditions (Muammar & Gupta, 1982; Petrus et al., 1998; Au et al., 2001; Baltzis & Sahalos, 2009b), we can express the average probability of outage of CCI as

$$P_{out} \underset{def}{=} P(CIR < Q) = \sum_{n=1}^{N} P(Z_d < 0 | n) P(n) \qquad (10)$$

As an example, Fig. 9 illustrates the outage curves of a WCDMA cellular system for different BS antenna half-power beamwidths. The antennas are flat–top beamformers; an example of an omni-directional one is also shown. In the simulations, the protection ratio is 8 dB and the activity level of the users equals to 0.4. Decrease in the beamformer's beamwidth up to a point reduces significantly the outage probability of co-channel interference indicating the

significance of sectorization and/or the use of narrow–beam base station transmission antennas.
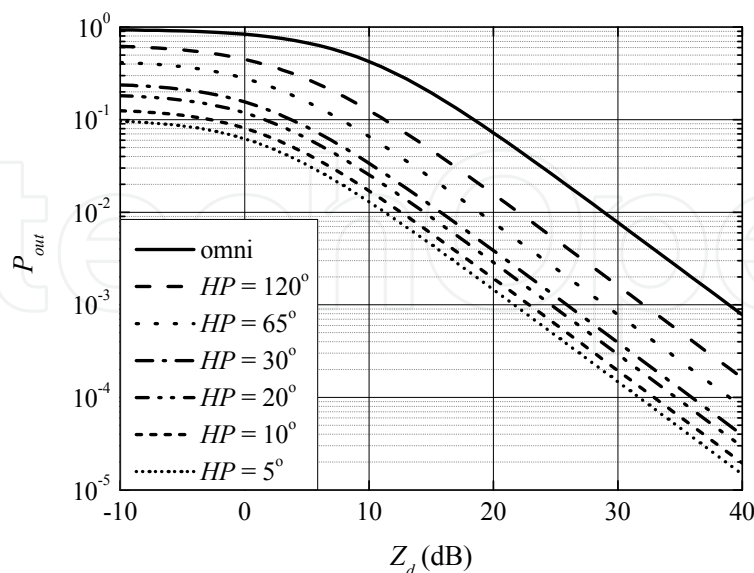

Fig. 9. Plot of outage curves as a function of *CIRP*.

In the calculation of co-channel interference, the inradius approximation considers part of the cell coverage area; on the contrary, the circumradius approach takes into account nodes not belonging to the cell, see Fig. 2. In both cases, an initial network planning that employs hexagonal cells but applies a circular model for the description of co-channel interference does not utilize network resources effectively. A hexagonal model is more accurate when network planning and design consider hexagonal–shaped cells. The comparisons we performed show that the inradius approximation compared with the circumradius one gives results closer to the hexagonal approach. In fact, it has been found that circles with radius that range between $1.05r$ and $1.1r$ give results closer to the hexagonal solution (Baltzis & Sahalos, 2010). Similar results are drawn for several other performance metrics (Oh & Li, 2001).

4. Cell shape and path loss statistics

In system-level simulations of wireless networks, path loss is usually estimated by distributing the nodes according to a known distribution and calculating the node-to-node distances. Thereafter, the application of a propagation model gives the losses. In order to increase the solution accuracy, we repeat the procedure many times but at the cost of simulation time. Therefore, the analytical description of path loss reduces significantly the computational requirements and may provide a good trade-off between accuracy and computational cost.

In the wireless environment, path loss increases exponentially with distance. The path loss at a distance d greater than the reference distance of the antenna far-field d_0 may be expressed in the log-domain (Parsons, 2000; Ghassemzadeh, 2004; Baltzis, 2009) as

$$L = L_0 + 10\gamma \log\left(d/d_0\right) + X_S + Y, \quad d > d_0 \tag{11}$$

where L_0 is the path loss at d_0, γ is the path loss exponent, X_S is the shadowing term and Y is the small-scale fading variation. Shadowing is caused by terrain configuration or obstacles

between the communicating nodes that attenuate signal power through absorption, reflection, scattering and diffraction and occurs over distances proportional to the size of the objects. Usually, it is modeled as a lognormal random process with logarithmic mean and standard deviation μ and σ, respectively (Alouini and Goldsmith, 1999; Simon and Alouini, 2005). Small-scale fading is due to constructive and destructive addition from multiple signal replicas (multipaths) and happens over distances on the order of the signal wavelength when the channel coherence time is small relative to its delay spread or the duration of the transmitted symbols. A common approach in the literature, is its modeling by the Nakagami-*m* distribution (Alouini and Goldsmith, 1999; Simon and Alouini, 2005; Rubio et al., 2007).

The combined effect of shadowing and small-scale fading can be modeled with the composite Nakagami-lognormal distribution. In this case, the path loss pdf between a node distributed uniformly within a circular cell with radius R and the center of the cell is (Baltzis, 2010b)

$$f_L(l) = \frac{1}{\xi\gamma R^2}\exp\left(2\left[\frac{l-L_0-\mu_C}{\xi\gamma}+\left(\frac{\sigma_C}{\xi\gamma}\right)^2\right]\right)\text{erfc}\left(\frac{l-L_0-10\gamma\log R-\mu_C}{\sqrt{2}\sigma_C}+\frac{\sqrt{2}\sigma_C}{\xi\gamma}\right) \qquad (12)$$

with $\xi = 10/\ln 10 \approx 4.343$, m the Nakagami fading parameter and

$$\begin{aligned}\mu_C &= \xi\left[\Psi(m)-\ln m\right]\\ \sigma_C^2 &= \sigma^2 + \xi^2\zeta(2,m)\end{aligned} \qquad (13)$$

where $\Psi(\cdot)$ is the Euler's psi function and $\zeta(\cdot,\cdot)$ is the generalized Reimann's zeta function (Gradshteyn & Ryzhik, 1994). In the absence of small-scale fading, (12) is simplified (Bharucha & Haas, 2008) into

$$f_L(l) = \frac{\ln 10}{bR^2}\exp\left(\frac{2b(l-L_0)\ln 10 + 2(\sigma\ln 10)^2}{b^2}\right)\text{erfc}\left(\frac{l-L_0-b\log R+\frac{2\sigma^2\ln 10}{b}}{\sqrt{2}\sigma}\right) \qquad (14)$$

where $b = 10\gamma$.

In the case of hexagonal instead of circular cells, the path loss pdf (in the absence of small-scale fading; the incorporation of this factor is a topic for a potential next stage of future work extension) is (Baltzis, 2010a)

$$f(l) = \frac{\pi\ln 10}{2\sqrt{3}br^2}\left\{\begin{array}{l}100^{(l-L_0)/b}\exp(N^2)\left[\text{erfc}\left(\frac{l}{\sqrt{2}\sigma}-M+N-S\right)-2\left[\begin{array}{l}\text{erf}\left(\frac{l}{\sqrt{2}\sigma}-M+N-S\right)\\-\text{erf}\left(\frac{l}{\sqrt{2}\sigma}-M+N-T\right)\end{array}\right]\right]\\[2em]-\frac{6}{\pi}\sum_{j=0}^{+\infty}\left(\begin{array}{l}\frac{|P_{2j}(0)|}{2j+1}r^{2j+1}\exp\left(\left[(j-1/2)N\right]^2\right)10^{-(2j-1)(l-L_0)/b}\\[1em]\times\left(\begin{array}{l}\text{erf}\left(-\frac{l}{\sqrt{2}\sigma}+M+S+(j-1/2)N\right)\\-\text{erf}\left(-\frac{l}{\sqrt{2}\sigma}+M+T+(j-1/2)N\right)\end{array}\right)\end{array}\right)\end{array}\right\} \qquad (15)$$

with $P_{2j}(x), j \in \mathbf{N}$ the Legendre polynomials of order $2j$, $M = 2^{-1/2}\sigma^{-1}L_0$, $N = \sqrt{2}\sigma b^{-1}\ln 10$, $S = 2^{-1/2}\sigma^{-1}b\log r$ and $T = 2^{-1/2}\sigma^{-1}b\log\alpha$. A closed-form approximation of this expression is

$$f(l) = \frac{\sqrt{3}\ln 10}{2br^2}\left(100^{(l-L_0)/b}\exp(N^2)\left(\begin{array}{c}\text{erfc}\left(\frac{l}{\sqrt{2}\sigma}-M+N-S\right)\\+\frac{\sqrt{3}}{\sqrt{3}-2}\left(\begin{array}{c}\text{erf}\left(\frac{l}{\sqrt{2}\sigma}-M+N-S\right)\\-\text{erf}\left(\frac{l}{\sqrt{2}\sigma}-M+N-T\right)\end{array}\right)\end{array}\right)\\-\frac{2r\exp(N^2/4)}{\sqrt{3}-2}10^{(l-L_0)/b}\left(\begin{array}{c}\text{erf}\left(\frac{l}{\sqrt{2}\sigma}-M-S+\frac{N}{2}\right)\\-\text{erf}\left(\frac{l}{\sqrt{2}\sigma}-M-T+\frac{N}{2}\right)\end{array}\right)\right) \tag{16}$$

A significant difference between the circular and the hexagonal cell models appears in the link distance statistics. The link distance pdf from the center of a circular cell with radius R to a spatially uniformly distributed node within it is (Omiyi et al., 2006)

$$f(d) = \frac{2d}{R^2}\text{U}(d)\text{U}(R-d) \tag{17}$$

The link distance pdf within a centralised hexagonal cell with inradius r and circumradius a is (Pirinen, 2006)

$$f(d) = \begin{cases} \frac{\pi d}{\sqrt{3}r^2}, & 0 \le d \le r \\ \frac{2\sqrt{3}d}{r^2}\left[\frac{\pi}{6}-\cos^{-1}\left(\frac{r}{d}\right)\right], & r \le d \le a \\ 0, & d \ge a \end{cases} \tag{18}$$

Figure 10 shows the link distance pdf and cdf curves for centralized hexagonal and circular cells. Notice the differences between the hexagonal and the circular approach. We further see that the inradius circular pdf and cdf are closer to the hexagonal ones compared with the circumradius curves.

Let us now consider a cellular system with typical UMTS air interface parameters (Bharucha & Haas, 2008). In particular, we set $\gamma = 3$ and $L_0 = 37$dB while shadowing deviation equals to 6dB or 12dB. The cells are hexagons with inradius 50m or 100m. Figure 11 shows the path loss pdf curves derived from (14)-(16). The corresponding cdfs, see Fig. 12, are generated by integrating the pdfs over the whole range of path losses. A series of simulations have also been performed for the cases we studied. For each snapshot, a single node was positioned inside the hexagonal cell according to (9). Then, the distance between the generated node and the center of the hexagon was calculated and a different value of shadowing was computed. After one path loss estimation using (11) (recall that small-scale fading was not considered), another snapshot continued. For each set of σ and r, 100,000 independent

simulation runs were performed. In Fig. 11, the simulation values were averaged over a path loss step-size of one decibel.

Figure 11 shows a good agreement between theory and simulation. We also notice that increase in σ flattens the pdf curve; as cell size increases the curve shifts to the right. The inradius approximation considers part of the network coverage area; as a result the pdf curve shifts to the left. The situation is reversed in the circumradius approximation because it considers nodes not belonging to the cell of interest. In practice, the first assigns higher probability to lower path loss values overestimating system performance. In this case, initial network planning may not satisfy users' demands and quality of service requirements. On the other hand, the circumradius approach assigns lower probability to low path loss values and underestimates system performance. As a result, network resources are not utilized efficiently. Again, the inradius approximation gives result closer to the hexagonal model.
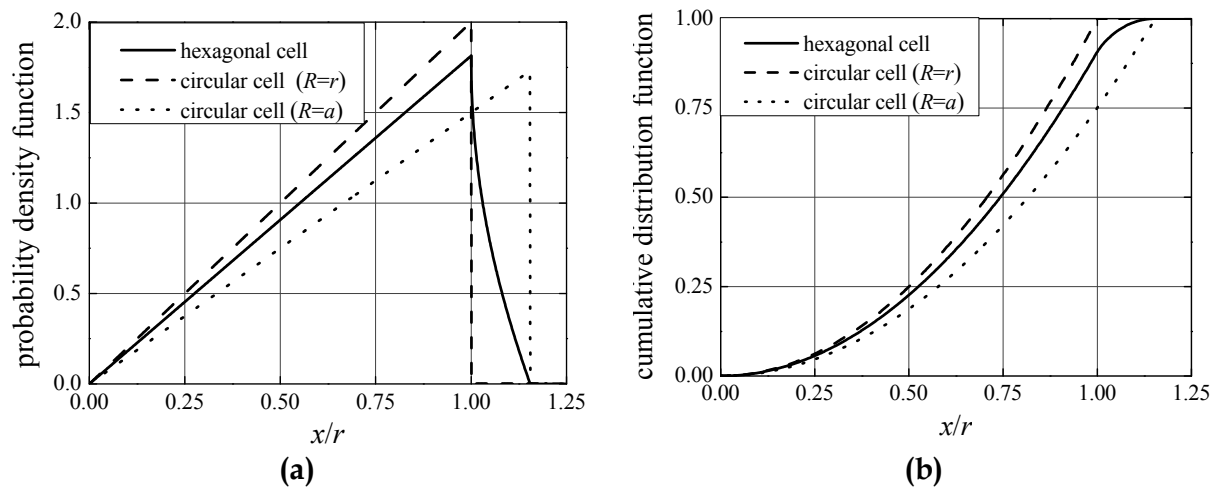

Fig. 10. Probability density function (a) and cumulative distribution function (b) curves.
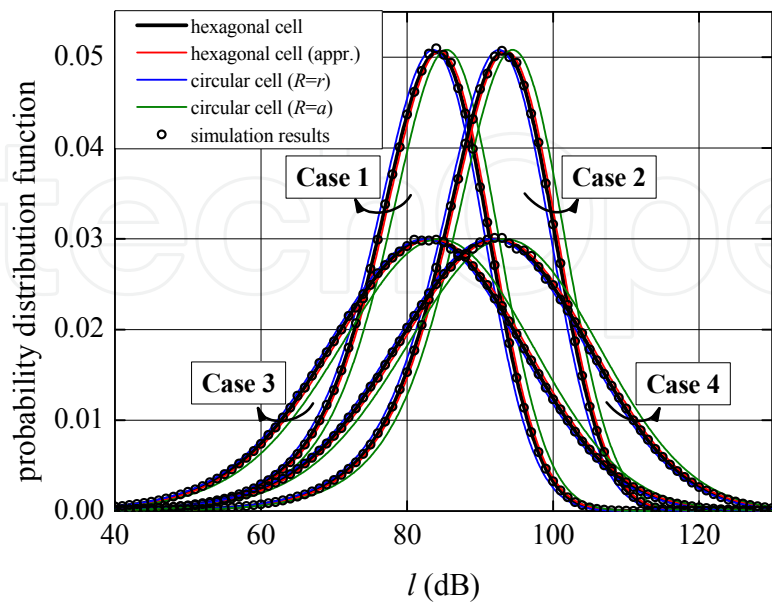

Fig. 11. Path loss pdf curves and simulation results; Case 1: $\sigma = 6\text{dB}$ and $r = 50\text{m}$; Case 2: $\sigma = 6\text{dB}$ and $r = 100\text{m}$; Case 3: $\sigma = 12\text{dB}$ and $r = 50\text{m}$; Case 4: $\sigma = 12\text{dB}$ and $r = 100\text{m}$.
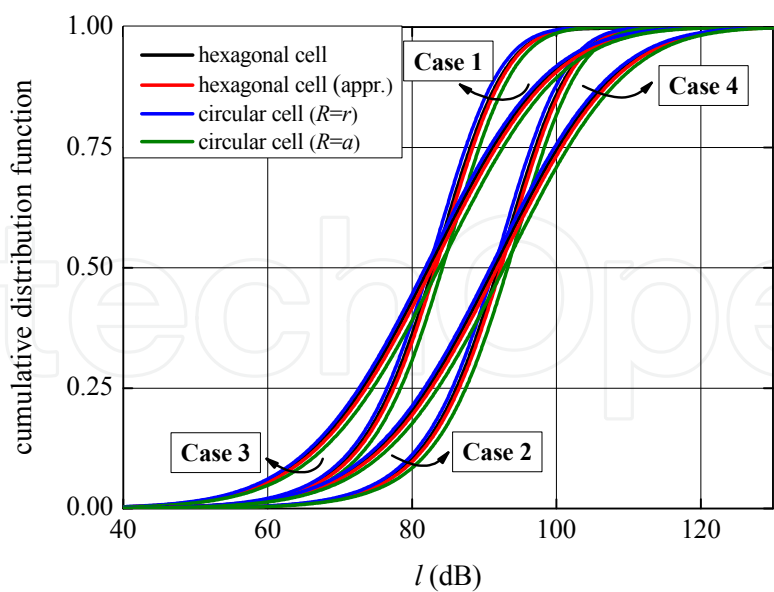
Fig. 12. Path loss cdf curves. (Cases 1 to 4 are defined as in Fig. 11).

Similar to before, we observe a good agreement between the hexagonal and the inradius circular approximation in Fig. 12. As it was expected, the curves shift to the right with cell size. However, the impact of shadowing is more complicated. Increase in σ, shifts the cdf curves to the left for path loss values up to a point; on the contrary, when shadowing deviation decreases the curves shift to the left with l. Moreover, Figs. 11 and 12 point out the negligible difference between the exact and the approximate hexagonal solutions.

Finally, Table 3 presents the predicted mean path loss values for the previous examples. The results show that the difference between the cell types is rather insignificant with respect to mean path loss. Notice also that the last does not depend on shadowing.

σ(dB)	r (m)	Mean path loss (dB)			
		hexagonal (15)	hexagonal (16)	inradius appr.	circumradius appr.
6	50	82.1	82.4	81.5	83.3
12	50	82.1	82.4	81.5	83.3
6	100	91.1	91.4	90.5	92.4
12	100	91.1	91.4	90.5	92.4

Table 3. Predicted mean path loss values.

A comparison between the proposed models and measured data (Thiele & Jungnickel, 2006; Thiele et al.; 2006) can be found in the literature (Baltzis, 2010a). In that case, the experimental results referred to data obtained from 5.2GHz broadband time-variant channel measurements in urban macro-cell environments; in the experiments, the communicating nodes were moving toward distant locations at low speed. It has been shown that the results derived from (15) and (16) were in good agreement with the measured data. The interested reader can also consult the published literature (Baltzis, 2010b) for an analysis of the impact of small-scale fading on path loss statistics using (12).

5. Research ideas

As we have stated in the beginning of this chapter, cells are irregular and complex shapes influenced by natural terrain features, man-made structures and network parameters. In most of the cases, the complexity of their shape leads to the adoption of approximate but simple models for its description. The most common modeling approximations are the circular and the hexagonal cell shape. However, alternative approaches can also be followed. For example, an adequate approximation for microcellular systems comprises square- or triangular-shaped cells (Goldsmith & Greenstein, 1993; Tripathi et al., 1998). Nowadays, the consideration of more complex shapes for the description of cells in emerging cellular technologies is of significant importance. An extension of the ideas discussed in this chapter in networks with different cell shape may be of great interest.

Moreover, in the models we discussed, several assumptions have been made. Further topics that illustrate future research trends include, but are not limited to, the consideration of non-uniform nodal distribution (e.g. Gaussian), the modeling of multipath uplink interfering signal, the use of directional antennas, the modeling of fading with distributions such as the generalized Suzuki, the *G*-distribution and the generalized *K*-distribution (Shankar; 2004; Laourine et al., 2009; Withers & Nadarajah, 2010), etc.

6. Conclusion

This chapter discussed, evaluated and compared two common assumptions in the modeling of the shape of the cells in a wireless cellular network, the hexagonal and the circular cell shape approximations. The difference in results indicated the significance of the proper choice of cell shape, a choice that is mainly based on system characteristics. In practice, use of the hexagonal instead of the circular–cell approximation gives results more suitable for the simulations and planning of wireless networks when hexagonal–shaped cells are employed. Moreover, it was concluded that the inradius circular approximation gives results closer the hexagonal approach compared to the circumradius one.

The chapter also provided a review of some analytical models for co-channel interference analysis and path loss estimation. The derived formulation allows the determination of the impact of cell shape on system performance. It further offers the capability of determining optimum network parameters and assists in the estimation of network performance metrics and in network planning reducing the computational complexity.

7. References

Aldmour, I. A.; Al-Begain, K. & Zreikat, A. I. (2007). Uplink capacity/coverage analysis of WCDMA with switched beam smart antennae. *Wireless Personal Communications*, Vol. 43, no. 4, Dec. 2007, 1705-1715

Almers, P. et al. (2007). Survey of channel and radio propagation models for wireless MIMO systems. *EURASIP Journal on Wireless Communications and Networking*, Vol. 2007, 19 pages, doi:10.1155/2007/19070

Alouini, M.-S. & Goldsmith, A. J. (1999). Area spectral efficiency of cellular mobile radio systems. *IEEE Transactions on Vehicular Technology*, Vol. 48, no. 4, July 1999, 1047-1066

Andrews, J. G.; Weber, S. & Haenggi, M. (2007). Ad hoc networks: To spread or not to spread?. *IEEE Communications Magazine*, Vol. 45, no. 12, Dec. 2007, 84-91

Au, W. S.; Murch, R. D. & Lea, C. T. (2001). Comparison between the spectral efficiency of SDMA systems and sectorized systems. *Wireless Personal Communications*, Vol. 16, no. 1, Jan. 2001, 51-67

Baltzis, K. B. (2008). A geometrical-based model for cochannel interference analysis and capacity estimation of CDMA cellular systems. *EURASIP Journal on Wireless Communications and Networking*, Vol. 2008, 7 pages, doi:10.1155/2008/791374

Baltzis, K. B. (2009). Current issues and trends in wireless channel modeling and simulation. *Recent Patents on Computer Science*, Vol. 2, no. 3, Nov. 2009, 166-177

Baltzis, K. B. (2010a). Analytical and closed-form expressions for the distribution of path loss in hexagonal cellular networks. *Wireless Personal Communications*, Mar. 2010, 12 pages, doi:10.1007/s11277-010-9962-2

Baltzis, K. B. (2010b). Closed-form description of microwave signal attenuation in cellular systems. *Radioengineering*, Vol. 19, no. 1, Apr. 2010, 11-16

Baltzis, K. B. & Sahalos, J. N. (2005). A 3-D model for measuring of the interference degradation of wireless systems, *Proceedings of Mediterranean Microwave Symposium 2005 (MMS'05)*, pp. 85-90, Athens, Sept. 2005

Baltzis, K. B. & Sahalos, J. N. (2009a). A simple 3-D geometric channel model for macrocell mobile communications. *Wireless Personal Communications*, Vol. 51, no. 2, Oct. 2009, 329-347

Baltzis, K. B. & Sahalos, J. N. (2009b). A low-complexity 3-D geometric model for the description of CCI in cellular systems. *Electrical Engineering (Archiv für Elektrotechnik)*, Vol. 91, no. 4-5, Dec. 2009, 211-219

Baltzis, K. B. & Sahalos, J. N. (2010). On the statistical description of the AoA of the uplink interfering signals in a cellular communications system. *European Transactions on Telecommunications*, Vol. 21, no. 2, Mar. 2010, 187-194

Bharucha, Z. & Haas, H. (2008). The distribution of path losses for uniformly distributed nodes in a circle. *Research Letters in Communications*, Vol. 2008, 4 pages, doi:10.1155/2008/376895

Bolton, W.; Xiao, Y. & Guizani, M. (2007). IEEE 802.20: mobile broadband wireless access. *IEEE Wireless Communications*, Vol. 14, no. 1, Feb. 2007, 84-95

Butterworth, K. S.; Sowerby, K. W. & Williamson, A. G. (2000). Base station placement for in-building mobile communication systems to yield high capacity and efficiency. *IEEE Transactions on Communications*, Vol. 48, no. 4, Apr. 2000, 658-669

Cardieri, P. & Rappaport, T. S. (2001). Application of narrow-beam antennas and fractional loading factors in cellular communication systems. *IEEE Transactions on Vehicular Technology*, Vol. 50, no. 2, Mar. 2001, 430-440

Cerri, G.; Cinalli, M.; Michetti, F. & Russo, P. (2004). Feed forward neural networks for path loss prediction in urban environment. *IEEE Transactions on Antennas and Propagation*, Vol. 52, no. 11, Nov. 2004, 3137-3139

Chan, A. & Liew, S. C. (2007). VoIP capacity over multiple IEEE 802.11 WLANs, *Proceedings of 2007 IEEE International Conference on Communications (ICC'07)*, pp. 3251-3258, Glasgow, June 2007

Cho, H.-S.; Kwon, J. K. & Sung, D. K. (2000). High reuse efficiency of radio resources in urban microcellular systems. *IEEE Transactions on Vehicular Technology*, Vol. 49, no. 5, Sep. 2000, 1669-1667

Choi, S.-O. & You, K.-H. (2008). Channel adaptive power control in the uplink of CDMA systems. *Wireless Personal Communications*, Vol. 47, no. 3, Nov. 2008, 441-448

Czylwik, A. & Dekorsy, A. (2004). System-level performance of antenna arrays in CDMA-based cellular mobile radio systems. *EURASIP Journal on Applied Signal Processing*, Vol. 2004, no. 9, 1308-1320

Demestichas, P.; Katidiotis, A.; Petromanolakis, D. & Stavroulaki, V. (2010). Management system for terminals in the wireless B3G world. *Wireless Personal Communications*, Vol. 53, no. 1, Mar. 2010, 81-109

Deng, L.-Y & Xu, H. (2003). A system of high-dimensional, efficient, long-cycle and portable uniform random generators. *ACM Transactions on Modeling and Computer Simulation*, Vol. 13, no. 4, Oct. 2003, 299-309

Dou, J.; Guo, Z.; Cao, J. & Zhang, G. (2008). Lifetime prolonging algorithms for wireless sensor networks, *Proceedings of 4th IEEE International Conference on Circuits and Systems for Communications (ICCSC 2008)*, pp. 833-837, Shanghai, May 2008

Fryziel, M.; Loyez, C.; Clavier, L.; Rolland, N. & Rolland, P. A. (2002). Path-loss model of the 60-GHz indoor radio channel. *Microwave and Optical Technology Letters*, Vol. 34, no. 3, Aug. 2002, 158-162

Fuhl, J.; Rossi, J.-P. & Bonek, E. (1997). High-resolution 3-D direction-of-arrival determination for urban mobile radio. *IEEE Transactions on Antennas and Propagation*, Vol. 45, no. 4, Apr. 1997, 672-682

Ghassemzadeh, S. S.; Jana, R.; Rice, C. W.; Turin, W. & Tarokh, V. (2004). Measurement and modeling of an ultra-wide bandwidth indoor channel. *IEEE Transactions on Communications*, Vol. 52, no. 10, Oct. 2004, 1786-1796

Gilhousen, K. S.; Jacobs, I. M.; Padovani, R.; Viterbi, A. J.; Weaver, L. A. Jr. & Wheatley, C. E. III (1991). On the capacity of a cellular CDMA system. *IEEE Transactions on Vehicular Technology*, Vol. 40, no. 2, May 1991, 303-312

Goldsmith, A. (2005). *Wireless Communications*, Cambridge University Press, New York

Goldsmith, A. J. & Greenstein, L. J. (1993). A measurement-based model for predicting coverage areas of urban microcells. *IEEE Journal on Selected Areas in Communications*, Vol. 11, no. 7, Sep. 1993, 1013-1023

Gradshteyn, I. S. & Ryzhik, I. M. (1994). *Table of Integrals, Series, and Products*, 5th ed., Academic Press, London

Grant, S. J. & Cavers, J. K. (2004). System-wide capacity increase for narrowband cellular systems through multiuser detection and base station diversity arrays. *IEEE Transactions on Wireless Communications*, Vol. 3, no. 6, Nov. 2004, 2072-2082

Haenggi, M. (2008). A geometric interpretation of fading in wireless networks: Theory and applications. *IEEE Transactions on Information Theory*, Vol. 54, no. 12, Dec. 2008, 5500-5510

Holis, J. & Pechac, P. (2008). Elevation dependent shadowing model for mobile communications via high altitude platforms in built-up areas. *IEEE Transactions on Antennas and Propagation*, Vol. 56, no. 4, Apr. 2008, 1078-1084

Hoymann, C.; Dittrich, M. & Goebbels, S. (2007). Dimensioning cellular multihop WiMAX networks, *Proceedings of 2007 IEEE Mobile WiMAX Symposium*, pp. 150-157, Orlando, Mar. 2007

Jan, R.-H.; Chu, H.-C. & Lee, Y.-F. (2004). Improving the accuracy of cell-based positioning for wireless systems, *Computer Networks*, Vol. 46, no. 6, Dec. 2004, 817-827

Jordan, M.; Senst, M.; Yang, C.; Ascheid, G. & Meyr, H. (2007). Downlink based intercell time synchronization using maximum likelihood estimation, *Proceedings of 16th IST Mobile and Wireless Communications Summit*, pp. 1-5, Budapest, July 2007, doi:10.1109/ISTMWC.2007.4299174

Kim, K. I. (1993). CDMA cellular engineering issues. *IEEE Transactions on Vehicular Technology*, Vol. 42, no. 3, Aug. 1993, 345-350

Kuchar, A.; Rossi, J.-P. & Bonek, E. (2000). Directional macro-cell channel characterization from urban measurements. *IEEE Transactions on Antennas and Propagation*, Vol. 48, no. 2, Feb. 2000, 137-146

Laourine, A.; Alouini, M.-S.; Affes, S. & Stéphenne, A. (2009). On the performance analysis of composite multipath/shadowing channels using the G-distribution. *IEEE Transactions on Communications*, Vol. 57, no. 4, Apr. 2009, 1162-1170.

Lee, J. S. & Miller, L. E. (1998). *CDMA Systems Engineering Handbook*, Artech House, Boston

Lu, K.; Qian, Y.; Chen, H.-H. & Fu, S. (2008). WiMAX networks: From access to service platform. *IEEE Network*, Vol. 22, no. 3, May-Jun. 2008, 38-45

MacDonald, V. H. (1979). The cellular concept. *The Bell System Technical Journal*, Vol. 58, no. 1, Jan. 1979, 15-41

Masmoudi, A. & Tabbane, S. (2006). Other-cell-interference factor distribution model in downlink WCDMA systems. *Wireless Personal Communications*, Vol. 36, no. 3, Feb. 2006, 245-475

Moraitis, N. & Constantinou, P. (2004). Indoor channel measurements and characterization at 60 GHz for wireless local area network applications. *IEEE Transactions on Antennas and Propagation*, Vol. 52, no. 12, Dec. 2004, 3180-3189

Muammar, R. & Gupta, S. (1982). Cochannel interference in high–capacity mobile radio systems. *IEEE Transactions on Communications*, Vol. 30, no. 8, Aug. 1982, 1973-1978

Nawaz, S. J.; Qureshi, B. H.; Khan, N. M. & Abdel-Maguid, M. (2010). Effect of directional antenna on the spatial characteristics of 3-D macrocell environment, *Proceedings of 2nd International Conference on Future Computer and Communication (ICFCC 2004)*, Vol. 1, pp. 552-556, Wuhan, May 2010

Nie, C.; Wong, T. C. & Chew, Y. H. (2004). Outage analysis for multi–connection multiclass services in the uplink of wideband CDMA cellular mobile networks, *Proceedings of 3rd International IFIP-TC6 Networking Conference*, pp. 1426-1432, Athens, May 2004

Niemelä, J.; Isotalo, T. & Lempiäinen, J. (2005). Optimum antenna downtilt angles for macrocellular WCDMA network. *EURASIP Journal on Wireless Communications and Networking*, Vol. 2005, no. 5, Oct. 2005, 816-827

Oh, S. W. & Li, K. H. (2001). Evaluation of forward–link performance in cellular DS–CDMA with Rayleigh fading and power control. *International Journal of Communication Systems*, Vol. 14, no. 3, Apr. 2001, 243-250

Omiyi, P.; Haas, H. & Auer, G. (2007). Analysis of TDD cellular interference mitigation using busy-bursts. *IEEE Transactions on Wireless Communications*, Vol. 6, no. 7, Jul. 2007, 2721-2731

Östlin, E.; Zepernick, H.-J. & Suzuki, H. (2010). Macrocell path-loss prediction using artificial neural networks. *IEEE Transactions on Vehicular Technology*, Vol. 59, no. 6, July 2010, 2735-2747

Panagopoulos, A. D.; Kritikos, T. D. & Kanellopoulos, J. D. (2007). Adaptive uplink power control in adjacent DVB-RCS networks: Interference statistical distribution, *Proceedings of IEEE 18th International Symposium on Personal, Indoor and Mobile Radio Communications (PIMRC'07)*, pp. 1-4, Athens, Sep. 2007, doi:10.1109/PIMRC.2007.4394408

Parsons, J. D. (2000). *The Mobile Radio Propagation Channel*, 2nd ed., John Wiley & Sons Ltd, Chichester

Petrus, P.; Ertel, R. B. & Reed, J. H. (1998). Capacity enhancement using adaptive arrays in an AMPS system. *IEEE Transactions on Vehicular Technology*, Vol. 47, no. 3, Aug. 1998, 717-727

Pirinen, P. (2006). Cellular topology and outage evaluation for DS-UWB system with correlated lognormal multipath fading, *Proceedings of IEEE 17th International Symposium on Personal, Indoor and Mobile Radio Communications (PIMRC'06)*, pp. 1-5, Helsinki, Sep. 2006, doi:10.1109/PIMRC.2006.254343

Popescu, I.; Nikitopoulos, D.; Constantinou, P. & Nafornita, I. (2006). Comparison of ANN based models for path loss prediction in indoor environments, *Proceedings of 64th IEEE Vehicular Technology Conference (VTC-2006 Fall)*, pp. 1-5, Montreal, Sep. 2006, doi:10.1109/VTCF.2006.43

Raeside, D. E. (1976). Monte Carlo principles and applications. *Physics in Medicine and Biology*, Vol. 21, no. 2, Mar. 1976, 181-197.

Rubio, L.; Reig, J. & Cardona, N. (2007). Evaluation of Nakagami fading behaviour based on measurements in urban scenarios. *AEU - International Journal of Electronics and Communications*, Vol. 61, no. 2, Feb. 2007, 135-138

Shankar, P. M. (2004). Error rates in generalized shadowed fading channels. *Wireless Personal Communications*, Vol. 28, no. 3, Feb. 2004, 233-238

Simon, M. K. & Alouini, M.-S. (2005). *Digital Communication over Fading Channels*, 2nd ed., John Wiley & Sons, Inc., Hoboken

Stavroulakis, P. (2003). *Interference Analysis and Reduction for Wireless Systems*, Artech House, Inc., Norwood

Thiele, L. & Jungnickel, V. (2006). Out-of-cell channel statistics at 5.2 GHz, *Proceedings of First European Conference on Antennas and Propagation (EuCAP 2006)*, pp. 1-6, Nice, Nov. 2006, doi:10.1109/EUCAP.2006.4584756

Thiele, L.; Peter, M. & Jungnickel, V. (2006). Statistics of the Ricean k-factor at 5.2 Ghz in an urban macro-cell scenario, *Proceedings of 17th IEEE International Symposium on Personal, Indoor and Mobile Radio Communications (PIMRC'06)*, pp. 1-5, Helsinki, Sep. 2006, doi:10.1109/PIMRC.2006.254301

Tripathi, N. D.; Reed, J. H. & VanLandingham, H. F. (1998). Handoff in cellular systems. *IEEE Personal Communications*, Vol. 5, no. 6, Dec. 1998, 26-37

Webb, W. (2007). *Wireless Communications: The Future*, John Wiley & Sons, Ltd, Chichester

Withers, C. S. & Nadarajah, S. (2010). A generalized Suzuki distribution. *Wireless Personal Communications*, Jul. 2010, 24 pages, doi:10.1007/s11277-010-0095-4.

Xiao, L.; Greenstein, L.; Mandayam, N. & Periyalwar, S. (2008). Distributed measurements for estimating and updating cellular system performance. *IEEE Transactions on Communications*, Vol. 56, no. 6, June 2008, 991-998.

Xylomenos, G.; Vogkas, V. and Thanos, G. (2008). The multimedia broadcast/multicast service. *Wireless Communications and Mobile Computing*, Vol. 8, no. 2, Feb. 2008, 255-265

Zhang, Z.; Lei, F. & Du, H. (2006). More realistic analysis of co-channel interference in sectorization cellular communication systems with Rayleigh fading environments, *Proceedings of 2006 International Conference on Wireless Communications, Networking and Mobile Computing (WiCom'06)*, pp. 1-5, Wuhan, Sep. 2004, doi:10.1109/WiCOM.2006.184

Zhang, Z.; Wei, S.; Yang, J. & Zhu, L. (2004). CIR performance analysis and optimization of a new mobile communication cellular configuration, *Proceedings of 4th International Conference on Microwave and Millimeter Wave Technology (ICMMT 2004)*, pp. 826-829, Beijing, Aug. 2004

Zhou, Y.; Chin, F.; Liang, Y.-C. & Ko, C.-C. (2001). Capacity of multirate multicell CDMA wireless local loop system with narrowbeam antenna and SINR based power control. *International Journal of Wireless Information Networks*, Vol. 8, no. 2, Apr. 2001, 99-108

Zhou, Y.; Chin, F.; Liang, Y.-C. & Ko, C.-C. (2003). Performance comparison of transmit diversity and beamforming for the downlink of DS-CDMA system. *IEEE Transactions on Wireless Communications*, Vol. 2, no. 2, Mar. 2003, 320-334
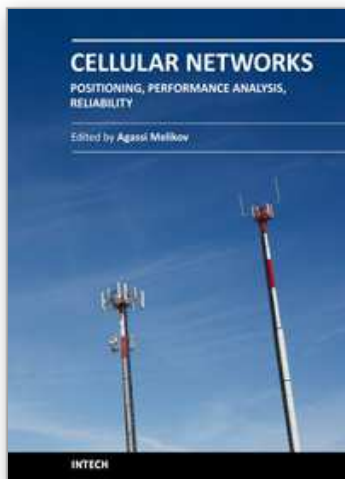
Cellular Networks - Positioning, Performance Analysis, Reliability

Edited by Dr. Agassi Melikov

Wireless cellular networks are an integral part of modern telecommunication systems. Today it is hard to imagine our life without the use of such networks. Nevertheless, the development, implementation and operation of these networks require engineers and scientists to address a number of interrelated problems. Among them are the problem of choosing the proper geometric shape and dimensions of cells based on geographical location, finding the optimal location of cell base station, selection the scheme dividing the total net bandwidth between its cells, organization of the handover of a call between cells, information security and network reliability, and many others. The book focuses on three types of problems from the above list - Positioning, Performance Analysis and Reliability. It contains three sections. The Section 1 is devoted to problems of Positioning and contains five chapters. The Section 2 contains eight Chapters which are devoted to quality of service (QoS) metrics analysis of wireless cellular networks. The Section 3 contains two Chapters and deal with reliability issues of wireless cellular networks. The book will be useful to researches in academia and industry and also to post-gradute students in telecommunication specialitiies.

How to reference

In order to correctly reference this scholarly work, feel free to copy and paste the following:

Konstantinos B. Baltzis (2011). Hexagonal vs Circular Cell Shape: A Comparative Analysis and Evaluation of the Two Popular Modeling Approximations, Cellular Networks - Positioning, Performance Analysis, Reliability, Dr. Agassi Melikov (Ed.), ISBN: 978-953-307-246-3, InTech, Available from: http://www.intechopen.com/books/cellular-networks-positioning-performance-analysis-reliability/hexagonal-vs-circular-cell-shape-a-comparative-analysis-and-evaluation-of-the-two-popular-modeling-a

INTECH
open science | open minds